

# Removal of Aspirin and Chloroquine from Aqueous Solution Using Organo-Clay Derived from Kaolinite

A.U. Nkwoada<sup>1\*</sup>, C.D. Alisa<sup>2</sup>, M.M. Oguwike<sup>3</sup>, I.A. Amaechi<sup>4</sup>

<sup>1,2,3,4</sup>Department of Chemistry, School of Physical Sciences, Federal University of Owerri, Imo State, Nigeria

\*Corresponding Author: amarachinkwoada@gmail.com, Tel.: +234 813 161 4206

Available online at: [www.isroset.org](http://www.isroset.org)

Received: 30/Jan/2022, Accepted: 03/Mar/2022, Online: 31/Mar/2022

**Abstract**—Common health problems such as malaria, fever and pain have made humans depend on drugs like chloroquine (Cq) and aspirin (Ap) for wellness. But these drugs and their metabolites invariably find their means to the environment and pollute our land and water; hence, suitable remediation technique is paramount to conserve our surroundings. Organo-clay synthesized by treating raw kaolinite with citric acid was explored as an adsorbent in this research paper. On the characterization of both raw clay and organo-clay using Fourier transform infrared (FTIR), X-ray diffraction (XRD) and scanning electron microscopy (SEM); the modification process resulted in structural and morphological changes. Employing batch adsorption for removal of Ap and Cq by organo-clay revealed that removal efficiency (R%) decreased with an increase in initial concentration (20–70mg/L), with the highest R% for Ap and Cq being 96.70% and 99.28%, respectively at 20mg/L. The contact time (5–120mins) for both Ap and Cq showed an increase in R% and then equilibration. The equilibrium time for Ap was 60min while Cq was 120min. The sorption isotherm investigated by both Freundlich and Langmuir models showed that both Ap and Cq follow the Langmuir model. The maximum sorption capacities of Ap and Cq onto organo-clay were 80.00 and 84.03mg/g, respectively. Among the kinetics models studied, namely, pseudo-first-order (PFO), pseudo-second-order (PSO), intraparticle diffusion (IDF) and Elovich, PSO describes the kinetics of both Ap and Cq onto organo-clay best based on correlation coefficient ( $R^2$ ) and also the sum of square error (SSE) values.

**Keywords**—Aspirin (Ap), Chloroquine (Cq), Adsorption, Treated Clay, Organo-Clay

## I. INTRODUCTION

The rapid development of certain pharmaceutical, chemical, petrochemical, agro-based, and textile industries has generated tremendous waste. Amongst these industries, chemical products in the form of drugs and their derivatives from pharmaceutical industries have been heavily distributed in land and water bodies [1, 2]. The common drug types detected are antidepressants, antibiotics, contraceptives, antiepileptics, anti-inflammatory, pain and fever relievers, and antimalaria. Most of these drug types, like Aspirin and Chloroquine, are well-known pharmaceutically active compounds (PACs). The concentration of PACs determined in land and water bodies is in the minute range (ngL<sup>-1</sup>) [3,4]; notwithstanding, continual discharging of pharmaceuticals for a long duration is a source of threat to the environment and living organisms. Aspirin has gained popularity due to its efficacy in treating fevers, aches and pains [5], whereas Chloroquine is commonly used in preventing and treating malaria [6]. With the outbreak of covid-19 in January 2020, Chloroquine has been reported as an effective drug for the treatment of COVID-19. With the rise in its synthesis, administration and continued use; Chloroquine and its metabolites invariably find their way into the environment [7].

The application of Aspirin and Chloroquine for various pharmaceutical purposes has led to a rise in the production of both drugs, increasing the amount present in wastewater effluents [7, 8]. These drugs find themselves in the environment via different routes. The primary route is drug use. After oral ingestion of these drugs, absorption and distribution follow; then bio-transformation (metabolization) and excretion of these drugs unchanged or as metabolites [9]. There is a good possibility that drugs like Aspirin and Chloroquine are directly excreted without any chemical alteration when taken in overdoses or at the wrong time. Other than the stated, 23 -25% of these drugs are excreted unmodified [10]. The metabolization process occurred by a biochemical pathway that transformed the original drug molecules [11]. The new products called "metabolites" are excreted and released into the natural environment and then transported to municipal sewage treatment plants, where they are treated using various techniques before being discharged [12]. Also, when faecal sludge is discharged in landfills, the leachate containing these PACs pass through the landfill barrier into groundwater and surrounding soil [13]. Additionally, effluents and waste disposal from hospitals and pharmaceutical industries runoff from dumpsites due to improper disposal of expired and unused drugs [14, 15].

PACs in effluents have noticeable effects in the environment as they undergo bio-concentration, microbial reduction, abiotic oxidation and reduction, which could raise the BOD and COD values of water bodies [16]. Also, some studies suggest that they could cause endocrine glands rupture, aquatic toxicity, the resistance of pathogenic micro-organism, carcinogenic cells development and genetic toxicity [17]. In particular, Aspirin in sufficient concentration readily acidifies water bodies. At the same time, Chloroquine, due to its chemical structure and physical and chemical properties, persists in the environment and can contaminate, bioaccumulate, and be transferred to living organisms in toxic forms [18]. Both Aspirin and Chloroquine are highly soluble in the aqueous system and recalcitrant to biodegradation, and as such, they both have raised serious concerns.

Rest of the paper is organized as follows, Section I contains the introduction of Aspirin and Chloroquine with respect to their effect on the ecosystem, Section II contain the related work of the current research work, Section III contain the methodology used in this work, Section IV contains the Results and Discussion of this research work, section V Concludes research work.

## II. RELATED WORK

Researchers have exploited various wastewater treatment techniques to mitigate the adverse consequences of PACs in the environment and living organisms [19]. Wastewater treatment methods studied could be broadly classified as biological, photo-chemical and physical. The biological wastewater treatment method utilizes micro-organisms and enzymes to cause the degradation of PACs and other organic pollutants. According to [20–22], biological methods have advantages such as environmental friendliness, degradation of pharmaceutical compounds, low cost but are insufficient and time-consuming to remove all potential poisons or contaminants present in wastewater. Advanced oxidation processes (AOPs), which involve the generation of very reactive species such as hydroxyl radicals  $\bullet\text{OH}$  that oxidize a wide broad-spectrum of pollutants readily and non-selectively, are used for removing recalcitrant organic matter from wastewater effluents degraded drugs by the aid of photolysis [23–24]; however, AOPs are costly and energy-consuming. Complete mineralization of pollutants is seldom attained, while toxic products or by-products may arise. Physical methods like membrane technologies, including reverse osmosis and ultrafiltration, have been exploited in organic contaminants removal [25]. Adsorption is an auspicious physical method of wastewater treatment. Currently, Activated Carbon (AC) has gained prominence for adsorbing PACs from wastewater due to its efficiency [26]; however, AC has limitations, such as high cost, pore-clogging, and hygroscopicity. Along with activated carbon, clay minerals have been investigated on their possible capacity to adsorb PACs [27]. Clays are fine-grained, natural, earthy, argillaceous materials. The particle size of clays is very fine and is generally considered to be about 2

$\mu\text{m}$  or less. The permeability of clay minerals is low, arising from compacted small grain particles. They also possess complex porous structures and large surface areas, which aid their interaction with organic and inorganic compounds [28].

Clay minerals such as montmorillonite, kaolin, fire clay, ball clay, bentonite and sepiolite have been investigated for their removal of organic pollutants. Among these candidates, kaolinite has been one of the most studied due to its cost-effectiveness, availability, and good sorption properties in removing active pharmaceutical ingredients (API) and auxiliary compounds in an aqueous medium [29]. In order to enhance the purity and adsorptivity of clay minerals on organic compounds, different researchers have used the term "treated" and "activated" to describe clay minerals that their adsorption capacities have been raised [29]. Another synthetic clay type unexplored in wastewater treatment is organo-clay; this clay type is synthesized by exchanging the original mineral interlayer cations for organo-cations [30]. To the best knowledge, no report has investigated the adsorption of PACs such as Chloroquine from wastewater effluent using organo-clay.

This study aims to probe the efficiency of treated clay and organo-clay and compare both in the adsorption of Aspirin and Chloroquine from aqueous solution.

## III. METHODOLOGY

### 3.1 Materials

All the solvent and chemical used was purchased from Sigma–Aldrich. The pharmaceutical products used as target adsorbate in the present study are Aspirin ( $\text{C}_9\text{H}_8\text{O}_4$ ) – purity  $\geq 98\%$  and Chloroquine ( $\text{C}_{18}\text{H}_{26}\text{ClN}_3$ ) – Purity  $>98.5\%$ . A stock solution of 1 g/L of Aspirin and Chloroquine each was prepared with distilled water. Every other reagent used is analytic grade. Sodium hydroxide (NaOH) and hydro chloric acid (HCl) were used for adjusting pH. Citric acid ( $\text{C}_6\text{H}_8\text{O}_7$ ) and ammonium hydroxide ( $\text{NH}_4\text{OH}$ ) were used for Organo-Clay preparation. 1 kg of Clay was obtained from Umuchi in Mbano.

### 3.2 Preparation of Treated Clay

About 12 g of raw Clay (C1) was mixed with 400 mL of deionized water for 12 hr. The mixture was centrifuged at 1000 rpm, 25 °C for 25 mins. Then, the final product being a supernatant was collected and dried at 85 °C overnight and named C2 [31].

### 3.3 Preparation of Organo-Clay

11.6 g of Clay was dissolved in 400 ml deionized water and added citric acid (3.8 g). The mixture was then stirred utilizing a magnetic stirrer for 1 hr. Furthermore, 10 mL of 50 % of ammonium hydroxide aqueous solution was added to obtain a pH of 7. Then the mixture was heated with a hot plate at 100°C for 2 hrs. Initially, a slurry gel appeared and finally a powder are obtained and named C3 [32].

### 3.4 Characterization

### 3.4.1 X-Ray Diffraction (XRD)

The C1 and C3 were analyzed by X-ray diffraction to determine the presence of crystalline minerals in raw Clay and to monitor the mineralogical changes caused by treatment; curves were recorded using copper radiation of wavelength  $\lambda = 0.154$  nm. The crushed materials were placed on metal plates. Measurements were carried out in an angular range of  $2\theta$  from  $0.03$  to  $80^\circ$ .

### 3.4.2 Scanning electron microscopy (SEM)

SEM has been used to determine the morphology and topography of both the raw and treated Clay. This was observed on a PHILIPS XL-30 FEG scanning electron microscope.

### 3.4.3 Fourier Transform Infrared Spectroscopy (FTIR)

The functional groups present in the samples was observed on a Fourier transform Infrared Spectroscopy by Transmittance method within the range of  $4000\text{--}650\text{cm}^{-1}$ .

### 3.5 Batch adsorption studies

Batch adsorption tests were carried out using the “bottle-point method”. A stock solution of Ap and Cq ( $1000\text{ mgL}^{-1}$ ) was prepared and then diluted to the needed initial concentrations. The adsorption capacity of the adsorbents onto Ap and Cq was deduced by contacting a constant mass ( $50\text{ mg}$ ) adsorbent with a fixed volume ( $100\text{ mL}$ ) in tight plastic bottles of initial concentrations from  $20$  to  $70\text{ (mgL}^{-1}\text{)}$  of Ap and Cq solution. The bottles were agitated in an isothermal water-bath shaker for  $24\text{ hr}$  until equilibrium was reached. Ap and Cq calibration curves were prepared by recording the absorbance values for a range of known concentrations of Ap and Cq solution. The maximum absorbance was determined ( $\lambda_{\text{max}} = 280\text{ nm}$  and  $\lambda_{\text{max}} = 340\text{ nm}$ , respectively); this was achieved using a double beam UV-visible spectrophotometer (UV-VIS) (Unico UV-2100). The quantity of Ap and Cq adsorbed onto adsorbent,  $q_e$  ( $\text{mgg}^{-1}$ ), was calculated by the following equation:

$$q_e = \frac{(C_0 - C_e)V}{m} \quad (1)$$

$$R\% = \frac{C_0 - C_e}{C_0} \times 100 \quad (2)$$

$$q_t = \frac{(C_0 - C_t)V}{w} \quad (3)$$

The  $C_0$ ,  $C_e$  and  $C_t$  depict Ap and Cq concentration ( $\text{mgL}^{-1}$ ) of the initial, equilibrium and at time ( $t$ ).  $V$  depicts the total volume of the adsorbate solution in litres, while  $m$  represents the mass ( $\text{g}$ ) of sorbent used.  $R\%$  depicts the removal efficiency (%Removal) [33].

### 3.6 Adsorption Isotherm

Adsorption isotherm was carried out at an initial concentration of Ap/Cq of  $20\text{ mg/L}$  solution and pH set at  $5.8$  using  $1\text{ M HCl}$  or  $1\text{ M NaOH}$ .  $5\text{ ml}$  of Ap/Cq solution was added to  $50\text{ mg}$  of Clay and agitated for the desired duration of  $50\text{ mins}$ . The mixture was afterwards centrifuged at  $5000\text{ rpm}$  for  $10\text{ mins}$  @  $25^\circ\text{C}$ . The concentration of the supernatant was measured by UV-

visible spectroscopy. Cq is expected at  $330/340\text{ nm}$ , while Ap is  $230/280\text{ nm}$ . The process was repeated for  $20, 30, 40, 50, 60, 70\text{ mg/L}$  concentrations of Aspirin and Cq. The amount of Ap/Cq adsorbed on the Clay was calculated (eqn 1) using the mass balance. Langmuir and Freundlich models were applied to describe the relationship between the adsorbed quantity of Ap and Cq and its equilibrium concentration in solution.

### 3.7 Batch adsorption kinetics

Adsorption kinetics was carried out at an initial concentration of Ap/Cq of  $0.5\text{ mg/mL}$  and pH set at  $5.8$  using  $1\text{ M HCl}$  or  $1\text{ M NaOH}$ .  $5\text{ ml}$  of Ap or Cq solution will be added to  $50\text{ mg}$  of clay and agitated for the desired duration of  $50\text{ mins}$ . Afterwards, the mixture will be centrifuged at  $5000\text{ rpm}$  for  $10\text{ minutes}$  @  $25^\circ\text{C}$ . The concentration of the supernatant was measured by UV-visible spectroscopy. Cq is expected at  $330/340\text{ nm}$ , while Ap is  $230/280\text{ nm}$ . The process was repeated for  $5, 10, 15, 30, 60, 120, 180\text{ mins}$  of agitation for Ap and Cq each. The amount of aspirin/chloroquine adsorbed on the Clay was calculated based on the mass balance. To investigate the adsorption characteristics of Ap and Cq on adsorbents (Treated and Organo-clay), Pseudo-first-order (PFO), Pseudo-second-order (PSO), Intraparticle diffusion (IPD) and Elovich were employed to examine the adsorption kinetics in this work [34, 35].

## IV. RESULTS AND DISCUSSION

### 4.1 Characterization

#### 4.1.1 XRD

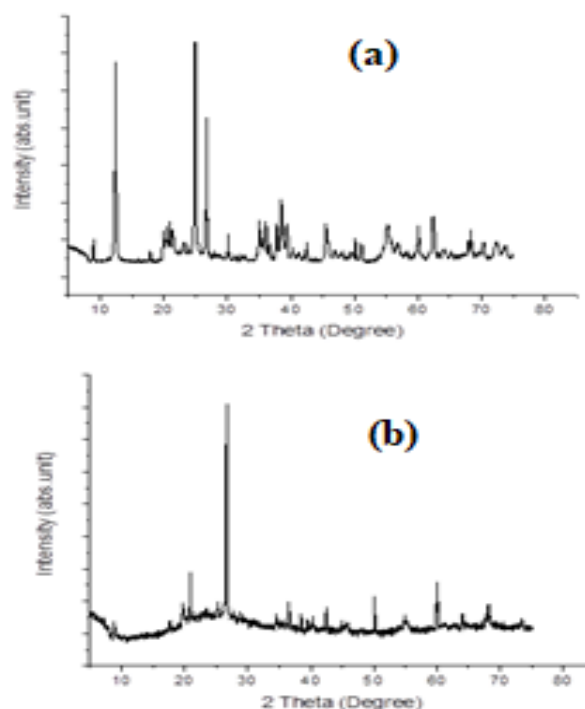


Figure 1: XRD diffractogram of (a) raw clay (b) treated clay

The X-Ray Diffraction graph for the raw clay (C1) showed 3 main peaks and other smaller peaks (Fig. 1a). At  $12^{\circ}$ ,  $26^{\circ}$  and  $27^{\circ}$ , respectively, the 3 main peaks for C1 was observed. For C3 (Fig. 1b), only one major peak was observed at  $27^{\circ}$ ; therefore, every other major peak observed in C1 remained, but the peak at  $27^{\circ}$ . This is owing to the raw clay's chemical treatment, which affected its structure, giving rise to only one major peak as opposed to 3 observed in C1 [36].

#### 4.1.2 FTIR

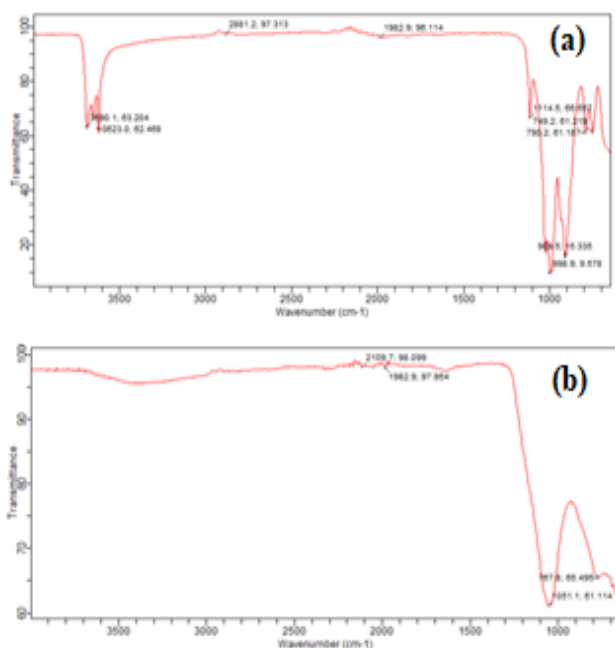


Figure 2: FTIR spectra (a) raw clay (b) treated clay

A complex molecule is observed from the FTIR chart for the clay sample's raw clay (Fig. 2a). A single bond region is evident, ranging from  $2500\text{-}4000\text{ cm}^{-1}$ . At  $3623\text{ cm}^{-1}$ , it confirms the existence of hydrogen bonding. This band confirms the presence of hydrate ( $\text{H}_2\text{O}$ ), hydroxyl ( $-\text{OH}$ ), ammonium, or amino group. The presence of spectra between  $1200\text{-}1000$  at  $1114.5\text{ cm}^{-1}$  with  $749.2$  and  $790.2$  in the range of  $800\text{-}600\text{ cm}^{-1}$  confirms the presence of a hydroxyl group. An aliphatic compound may be present as a narrow band below  $3000\text{ cm}^{-1}$  at  $2881.2\text{ cm}^{-1}$ . At  $1114.5$ ,  $749.2$  and  $790.2$ , which falls between the ranges of  $1300\text{-}700$ , a saturated aliphatic compound is observed, methyne most probably with a skeletal C-C vibration. A vinyl compound is observed at  $909.5$  as it falls between  $915\text{-}890$ , showing vinyl C-H out-of-plane bend. At  $1114.5$ , an aliphatic Fluoro compound is also observed with C-F stretch as it falls between  $1150\text{-}1000$  [37].

A simple spectrum is observed from the FTIR chart for organo-clay (Fig. 2b) as the peaks are fewer. At  $1051\text{ cm}^{-1}$ , a methylene group is evident as it falls within  $1055\text{-}1000\text{ cm}^{-1}$ , possibly a cyclohexane ring vibration peak. At  $767.8\text{ cm}^{-1}$ , a skeletal C-C vibration is observed, showing the presence of a methyne group as it falls between the range of  $1300\text{-}700\text{ cm}^{-1}$ . At  $1982.9$ , an aromatic

combination band is observed, possibly an aryl as it falls within  $2000\text{-}1660\text{ cm}^{-1}$ . A mono-substituted terminal alkyne is observed at  $2109.7$  as it falls within  $2140\text{-}2100\text{ cm}^{-1}$  [38]. Moreover both XRD and FTIR suggest a kaolinite clay mineral.

#### 4.1.3 SEM

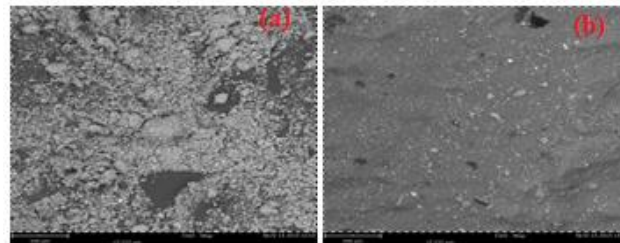


Figure 3: SEM micrograph (a) raw clay (b) organo-clay

The Scanning Electron Microscopy (SEM) gives the magnified images of a specimen's size, shape, composition, crystallography, and other physical and chemical properties. Scanning electron microscopy analysis allows visualization of the morphology of the studied materials, as shown in the figure above [39, 40]. Fig 3(a) below shows that the raw clay (C1) has fine structures, pores, slightly dispersed and agglomerated. The Organo-clay (C3) in fig 3(b) shows a kaolinite with finer layered surfaces, porous, more dispersed and homogenous distribution. C3 hence has a larger surface area to volume ratio than C1. These changes are significant and desirable for optimum adsorption performance by C3.

#### 4.2 Effect of Initial Aspirin and Chloroquine Concentration

The initial concentration is a critical parameters influencing Ap and Cq adsorption. In this respect, a series of batch experiments of Ap and Cq adsorption ( $\text{Co}$ :  $30\text{-}70\text{ mgL}^{-1}$ ) were carried out for a clay dose of  $0.05\text{ gL}^{-1}$  at pH 2 (fig. 4 and fig. 5) for both the C2 and C3.

Fig 4 shows the excellent performance of the C2 and C3 at equilibrium state and clarifies the optimum drug initial concentration used at confined experimental conditions. It is also evidently observed that the percentage removal of the Ap drug is sufficiently high,  $95.31\%$  and  $96.70\%$  for C2 and C3, respectively, at low concentration ( $20\text{ mg/L}$ ), and the removal efficiency decreases as initial concentration increases [41]. Fig 4 also shows that the optimum percentage removal of C3 is  $1.39\%$  higher than that of C2 for Ap adsorption.

Figure 5 also shows the excellent performance of the C2 and C3 at equilibrium state and clarifies the optimum drug initial concentration used at confined experimental conditions. It is also evidently observed that the percentage removal of the Cq drug is sufficiently high,  $97.30\%$  and  $99.28\%$  for C2 and C3, respectively, at low concentration ( $20\text{ mg/L}$ ), and the removal efficiency decreases as initial concentration increases. Fig 5 also also showed that the optimum percentage removal of Organo-clay is  $1.98\%$  higher than that of C2 for Cq adsorption.

The decrease in removal efficiency as the initial concentration increases for both the C2 and C3 in both Ap and Cq adsorption is because the equivalent molecular adsorption sites on the adsorbent surface were available for the increasing Adsorbate (Ap and Cq) concentration. This resulted into the overlapping of the adsorption sites on both the C2 and C3 adsorbent [42].

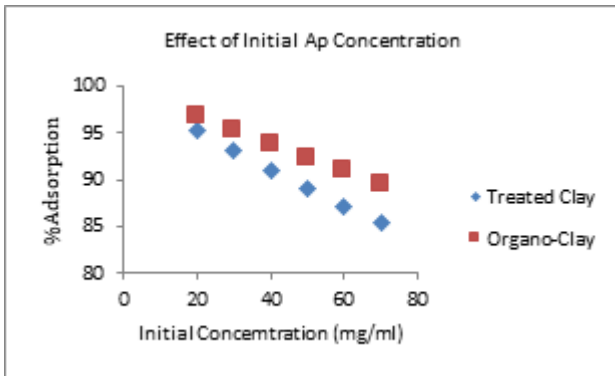


Figure 4: Effect of Initial Ap concentration on treated clay and organo-clay

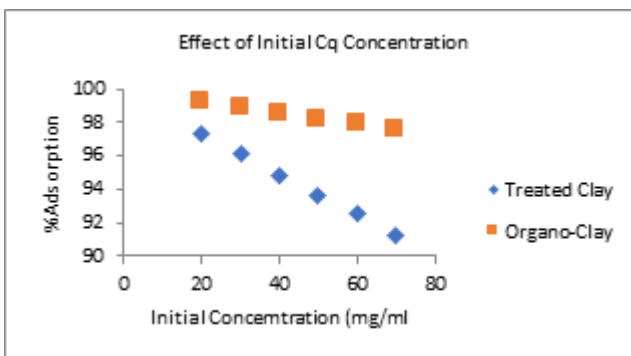


Figure 5: Effect of initial Cq concentration on treated clay and organo-clay

#### 4.3 Effect of Aspirin and Chloroquine Contact Time

The effect of contact time of the adsorbent in the adsorbate solution was investigated considering its real-life application in wastewater treatment. The contact time was studied at a standard condition of 0.2 mg/mL initial concentration, solution pH of 5.8, and temperature of 293 K at contact times of 5, 10, 15, 30, 60, and 240 min for Ap and Cq as shown in Fig 6 and 7. The result revealed rapid adsorption of both Ap and Cq by C2 and C3 in the first 15 to 30 minutes. From Fig. 6, C2 had a fast uptake of Ap and Cq in the initial 15 min and by 30 min constancy was almost observed in the % removal of Ap due to equilibration of adsorbate/adsorbent was attained while Cq took longer time to saturate the active sites of C2. Very similar trend was seen with C3 (Fig. 7) with the primary difference being that the % removal of C3 was comparatively higher in C3 than in C2 for both Ap and Cq at all contact times. The most suitable postulate for the rapid uptake in the first 30 min is due to the availability of active sites on the adsorbents and high concentration gradient at the start of adsorption [43]. As the adsorption continues, saturation occurs because of the unavailability

of active sites on the adsorbents and due to electrostatic repulsion between adsorbate molecules [44]. C3 had better % removal because C3 by treatment has become intercalated than C2; that is, the inorganic interlayer cations of the clay have been interchanged for organic cations and contain more adsorbable active sites.

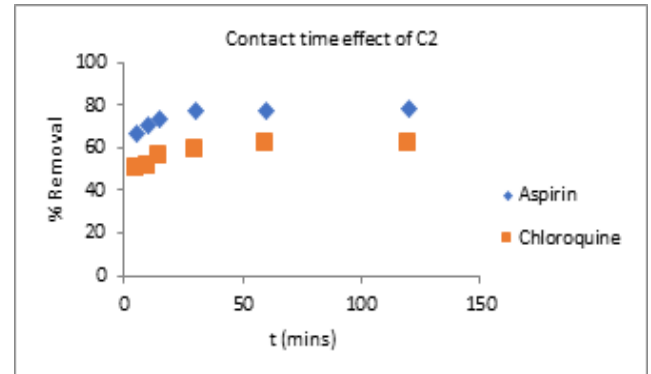


Figure 6: Effect of contact time of treated clay

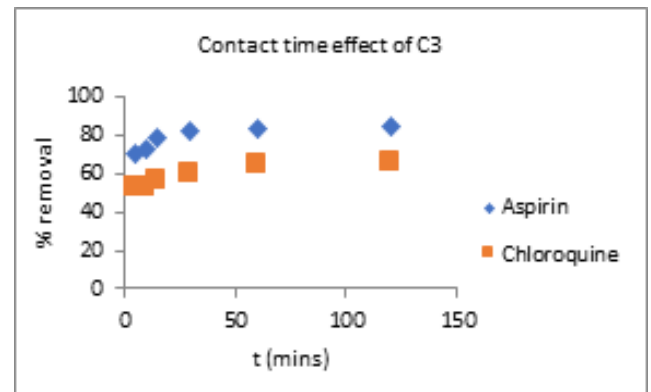


Figure 7: Effect of contact time of organo-clay

#### 4.4 Adsorption Isotherms

To describe the removal mechanism of Aspirin and Chloroquine onto the C2 and C3, two isotherm models (Freundlich and Langmuir) were applied to establish the relationship between the amount of adsorbed Aspirin and Chloroquine and their equilibrium concentration. The Langmuir isotherm is depicted by Eq. (4) [45].

$$\frac{c_e}{q_e} = \frac{1}{bLQ_{max}} + \frac{c_e}{Q_{max}} \quad (4)$$

$C_e$  is the supernatant concentration after the equilibrium of the system ( $\text{mgL}^{-1}$ ),  $bL$  depicts Langmuir affinity constant ( $\text{Lmg}^{-1}$ ), and  $Q_{max}$  depicts the maximum adsorption capacity of the material ( $\text{mgg}^{-1}$ ).

The Freundlich isotherm is depicted by Eq. (5) [46].

$$\ln q_e = \ln K_F + \frac{1}{n} \ln C_e \quad (5)$$

$K_F$  depicts the Freundlich constant ( $\text{Lg}^{-1}$ ), and  $n$  depicts the heterogeneity factor. The  $K_F$  value is related to the adsorption capacity, whereas the  $1/n$  value is linked to the adsorption intensity. The magnitude of ( $n$ ) is an indicator

of the favorability and capacity of the system and the value of (n) greater than unity represents favorable adsorption [47].

#### 4.4a. Adsorption Isotherms for Aspirin adsorption onto Treated Clay (C2) and Organo-clay (C3).

The values of  $Q_{max}$ ,  $K_L$ ,  $K_F$ , and  $n$  calculated from the Langmuir and Freundlich models for the adsorption of Ap onto C2 and C3 are presented in Table 1. The sorption of Ap onto both adsorbents is well fitted with the Langmuir sorption isotherm since the correlation coefficients for the Langmuir sorption of Ap were found to be 0.9806 and 0.9938 for C2 and C3, respectively (Figure 8, and 9), which are close to unity. The calculated  $Q_{max}$  and  $K_L$  values for the removal of Ap by C2 are 74.627  $\text{mgg}^{-1}$  and 0.0760  $\text{Lmg}^{-1}$ , respectively (fig. 8). The values for C3 are 80  $\text{mgg}^{-1}$ , 0.0218  $\text{Lmg}^{-1}$ , respectively (fig. 9). Comparison of the calculated  $Q_{max}$  values of Ap using C2 and C3 reveals that the C3 is more efficient than the C2 in removing Ap. The results can be explained by the means of physicochemical properties of the adsorbents, that is, water solubility [48]. This property can play a major role in the mobility of the drug in the subsurface adsorbents. The C3 has a more adsorptive effect when compared to C2. This adsorptive property makes Aspirin accumulate more onto C3 than it does with C2.

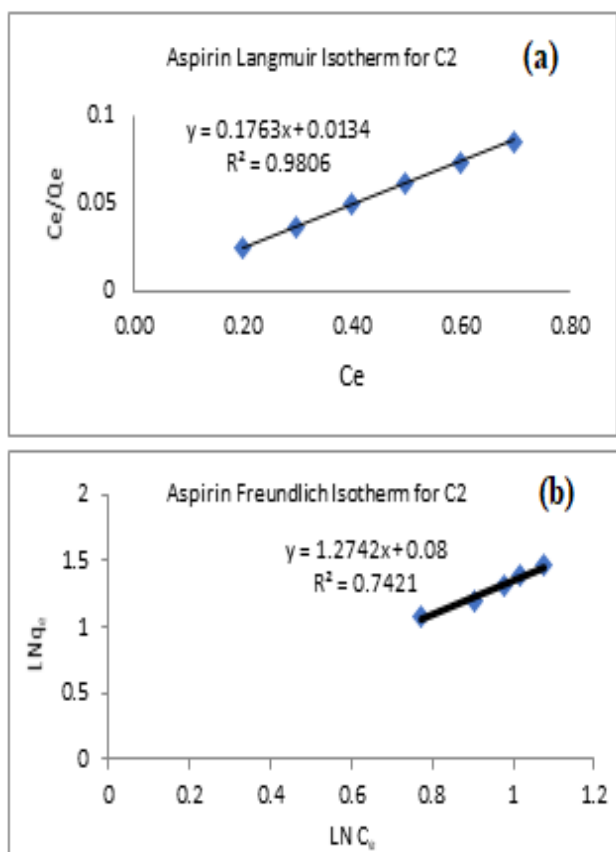


Figure 8: (a) Langmuir and (b) Freundlich adsorption isotherm of aspirin onto treated clay (C2)

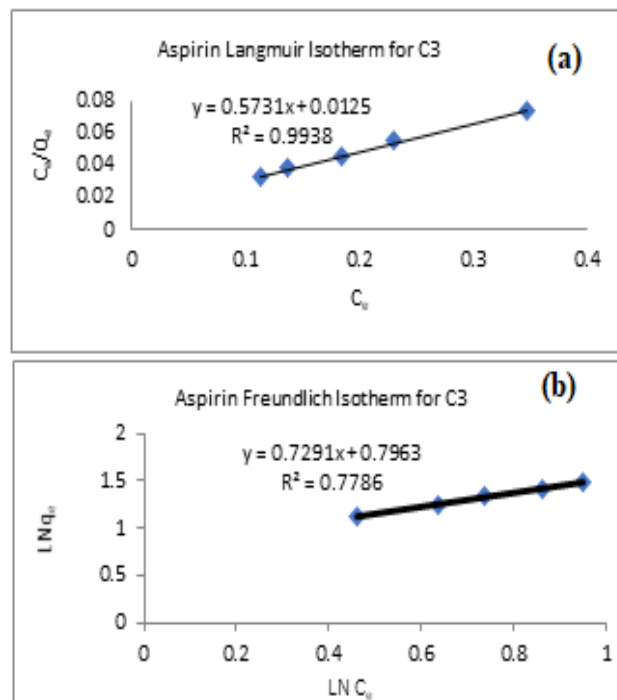


Figure 9 (a) Langmuir and (b) Freundlich adsorption isotherm of aspirin onto organo-clay (C3)

Table 1: The Langmuir and Freundlich isotherms parameters for the adsorption of Aspirin

Aspirin Isotherm Models	Parameters	C2	C3
Langmuir	$q_{max}(\text{mg/g})$	74.627	80
	$K_L(\text{L/mg})$	0.0760	0.0218
	$R^2$	0.9806	0.9938
Freundlich	$K_F$ ( $\text{mg}^{1-1/n}$ $\text{L}^{1/n} \text{g}^{-1}$ )	1.2023	6.2560
	$N$	0.7848	1.3716
	$R^2$	0.7421	0.7786

#### 4.4b. Adsorption Isotherms for Chloroquine (Cq) adsorption onto Treated clay (C2) and Organo-clay (C3).

The values of  $Q_{max}$ ,  $K_L$ ,  $K_F$ , and  $n$  calculated from the Langmuir and Freundlich models for the adsorption of Cq onto C2 and C3 are presented in Table 2. The sorption of Cq onto both adsorbents is well fitted with Langmuir sorption isotherm since the correlation coefficients for the Langmuir sorption of Cq were found to be 0.9905 and 0.9989 for C2 and C3, respectively (Fig 10 and 11), which are close to unity. The calculated  $Q_{max}$  and  $K_L$  values for the removal of Cq by C2 are 54.945  $\text{mgg}^{-1}$  and 0.0821  $\text{Lmg}^{-1}$ , respectively (fig. 10). The values for C3 are 84.034  $\text{mgg}^{-1}$ , 0.0803  $\text{Lmg}^{-1}$ , respectively (fig. 11). Comparison of the calculated  $Q_{max}$  values of Cq using C2 and C3 reveals that the later is more efficient than the former in removing Cq. The C3 has more adsorptive effect compared to C2. This adsorptive property makes Cq amass more onto C3 than it does with C2 [49].

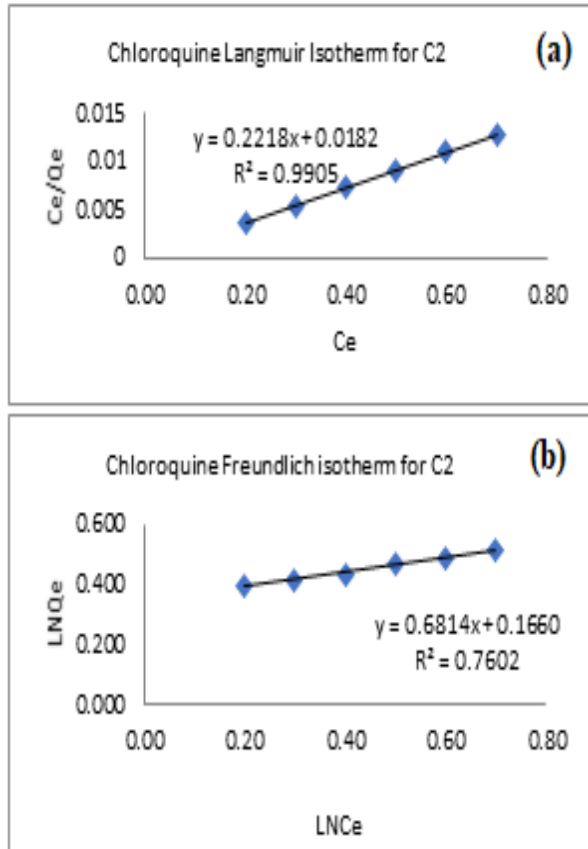


Figure 10: (a) Langmuir and (b) Freundlich adsorption isotherms of chloroquine onto treated clay (C2)

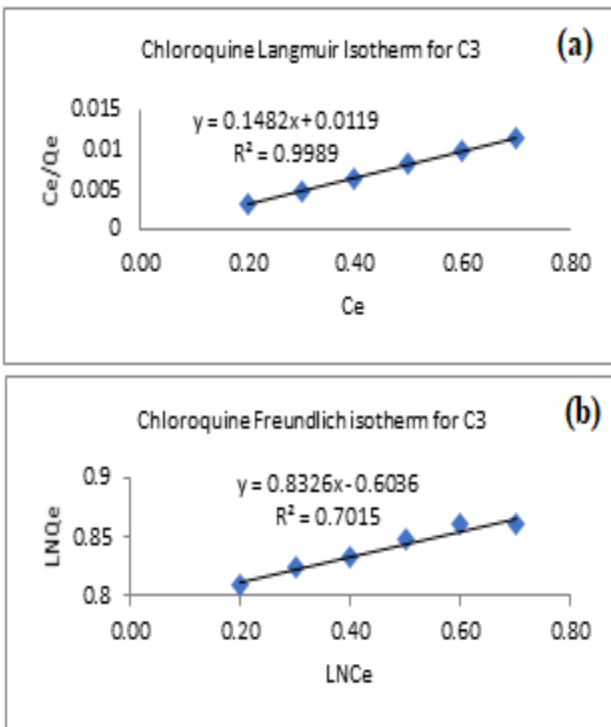


Figure 11: (a) Langmuir (b) Freundlich adsorption isotherms of chloroquine onto organo-clay (C3)

Table 2: The Langmuir and Freundlich Isotherms parameters for the adsorption of chloroquine

Chloroquine Isotherm Models	Parameters	C2	C3
Langmuir	$q_{\max}$ (mg/g)	54.945	84.034
	$K_L$ (L/mg)	0.0821	0.0803
	$R^2$	0.9905	0.9989
Freundlich	$K_F$ ( $\text{mg}^{1-1/n}$ $\text{L}^{1/n} \text{g}^{-1}$ )	1.466	0.249
	$N$	1.468	1.201
	$R^2$	0.7602	0.7015

#### 4.5 Adsorption Kinetics

To investigate the rate of reaction and the mechanism or sequence by which a reaction occurs, can be fundamental in the design of industrial sorption process technologies 1; four adsorption kinetic models were employed, namely; Pseudo first order (PFO), Pseudo second order (PSO), Intraparticle diffusion (IPD) and Elovich (Eqs. 6–9):

$$\ln(q_e - q_t) = \ln q_e - k_1 t \quad (6)$$

$$\frac{t}{q_t} = \frac{1}{k_2 q_e^2} + \frac{t}{q_e} \quad (7)$$

$$q_e = k_i t^{1/2} + c \quad (8)$$

$$q_t = \frac{1}{\beta} \ln \alpha \beta + \frac{1}{\beta} \ln t \quad (9)$$

Where  $t$  (min) is time,  $k_1$  ( $\text{min}^{-1}$ ),  $k_2$  ( $\text{g}/\text{mg}\cdot\text{min}$ ), and  $k_i$  ( $\text{g}/\text{mg}\cdot\text{min}$ ) are the rate constant of pseudo first-order sorption, rate constant of pseudo-second-order sorption and the intraparticle diffusion rate constant respectively;  $q_e$  ( $\text{mg}/\text{g}$ ) and  $q_t$  ( $\text{mg}/\text{g}$ ) are the amounts of PAC adsorbed at equilibrium ( $\text{mg}/\text{g}$ ) and at time  $t$ ;  $\alpha$  ( $\text{g}/\text{mg}\cdot\text{min}$ ) and  $\beta$  ( $\text{mg}/\text{g}$ ) are the initial adsorption rate and desorption constant; while  $c$  ( $\text{mg}/\text{g}$ ) is a constant that provides information about thickness of the boundary layer [50, 51].

The various plots for the models are presented in Fig. 12 to 15, and the evaluated parameters are shown in tables 3 to 4 for aspirin and chloroquine. From the results, PFO poorly fits the sorption of both PACS as the  $q_e$  (exp) and  $q_e$  (cal) are far apart. The  $R^2$  values ranging from 0.6991 to 0.8690 indicate poor correlation of scientific data, and the large SSE values indicate more significant errors. While PSO illustrates best the adsorption of Ap and Cq onto C3, the  $q_e$  (exp) and  $q_e$  (cal) are much identical. The  $R^2$  values (0.9321 - 0.9978) clearly show a more excellent data correlation, and the SSE value (0.0121 - 0.0891) indicates minimum errors. The decreasing  $k_2$  for increasing concentration indicates that adsorption capacities will decline due to less active site on the adsorbent; this observation was also made by [51]. The results show that

for a solid/liquid sorption process such as adsorption of Ap and Cq onto C3, intraparticle diffusion was also involved [52]. However, since the graph for IPD did not pass through the origin, IDP is not the rate-determining step; hence, the sorption is influenced by mass transfer and intraparticle diffusion [53]. Also,  $k_i$  increased with increasing concentration indicating percolation of Ap and Cq into C3. The Elovich model has lower  $R^2$  and higher SSE, suggesting that the model is less suitable for the kinetic data. The change of non-linear equations into a linear one generally changes the degree and pattern in their error [54]. So the sum of the square of errors (SSE) and correlation coefficient ( $R^2$ ) are the decisive parameters for adsorption kinetic. Table 3 and 4 PSO best describe the kinetics for both Ap and Cq. Though not presented here, PSO kinetics best fits both Ap and Cq adsorption using C2 but with lower  $q_e$ .

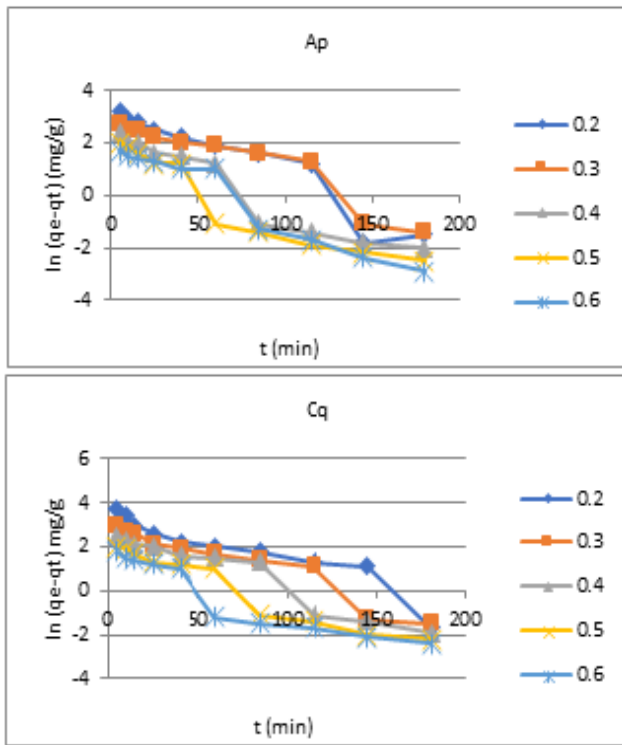


Figure 12: Pseudo first order in Ap and Cq

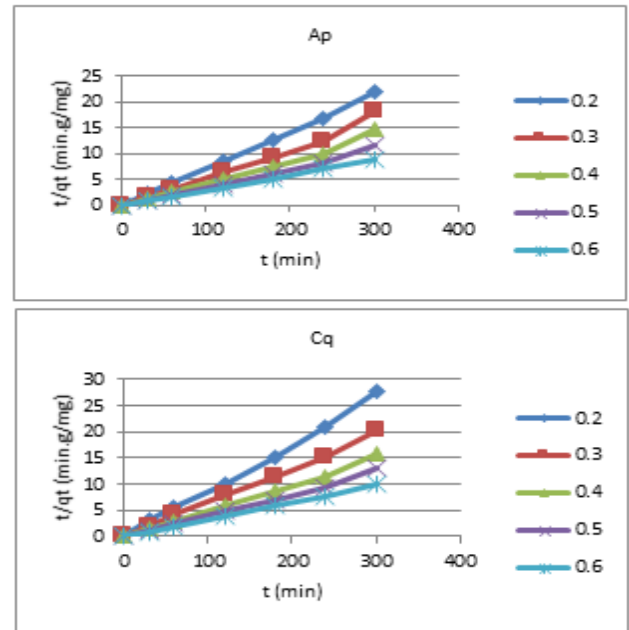


Figure 13: Pseudo second order in Ap and Cq

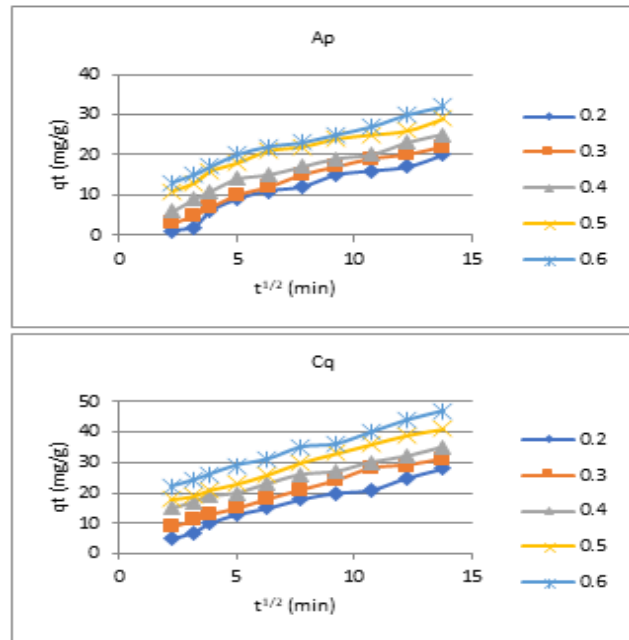


Figure 14: Intraparticle diffusion (IPD) for Ap and Cq

Table 3: Aspirin kinetic parameters

Model	Parameter	20	30	40	50	60
PFO	$q_e$ (exp) mg/g	10.8871	15.0117	21.7609	28.1826	40.3231
	$q_e$ (cal) mg/g	15.9003	29.0191	35.3318	42.8817	50.3232
	$k_1$ (min <sup>-1</sup> )	0.0321	0.0110	0.0440	0.0413	0.0137
	$R^2$	0.8312	0.7951	0.8690	0.6991	0.7018
	SSE	2.3456	3.1109	1.3421	2.9192	1.0345
PSO	$q_e$ (cal) mg/g	10.0019	16.0119	21.4321	29.4101	40.0997
	$k_2$ (g/mg.min)	0.0775	0.0721	0.0692	0.0655	0.0601
	$R^2$	0.9543	0.9321	0.9978	0.9521	0.9891
	SSE	0.0312	0.0121	0.0351	0.0223	0.0891
IPD	$k_i$ (g/mg.min)	0.4173	0.5213	0.8231	1.3002	3.4038
	C (mg/g)	5.77781	7.8910	11.6911	18.1710	20.7723
	$R^2$	0.8129	0.8413	0.8891	0.9009	0.9121
	SSE	0.2424	0.4512	0.6637	0.8123	0.9981



Elovich	$\alpha$ (g/mg.min)	20.1451	17.3321	12.5211	8.7621	4.3241
	$\beta$ (mg/g)	0.1456	0.2341	0.4423	0.5778	0.8821
	$R^2$	0.8126	0.8401	0.8891	0.9009	0.9121
	SSE	0.0935	0.07802	0.0678	0.0884	0.0982

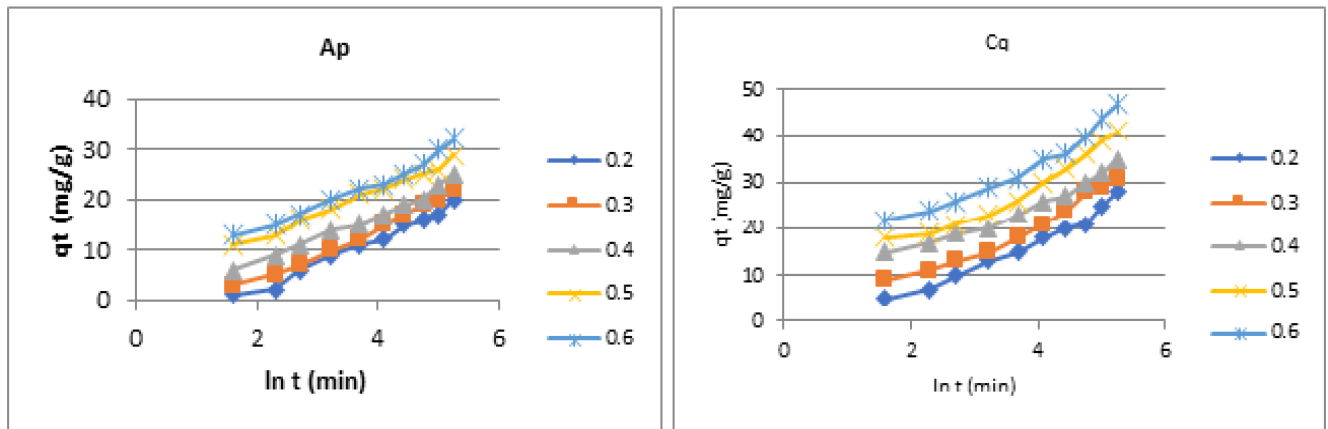


Figure 15: Elovich plot for Ap and Cq

Table 4: Chloroquine kinetic parameters

Model	Parameter	20	30	40	50	60
PFO	$q_e$ (exp) mg/g	4.7811	6.3214	7.1218	10.0011	9.3214
	$q_e$ (cal) mg/g	8.8412	14.6211	18.7721	24.3011	25.9321
	$k_1$ (min <sup>-1</sup> )	0.1124	0.1245	0.3321	0.5171	0.4424
	$R^2$	0.7521	0.7991	0.8211	0.8521	0.8001
	SSE	0.1124	0.1234	0.3211	0.8902	0.2114
PSO	$q_e$ (cal) mg/g	5.7811	7.3214	7.9249	10.8101	10.1192
	$k_2$ (g/mg.min)	0.0774	0.0621	0.0491	0.0412	0.0245
	$R^2$	0.9121	0.9551	0.9972	0.9910	0.9521
	SSE	0.0811	0.0897	0.0942	0.0992	0.1451
IPD	$k_i$ (g/mg.min)	0.0056	0.0072	0.0099	0.0321	0.0481
	C (mg/g)	2.4567	3.8214	6.7811	7.4266	8.2245
	$R^2$	0.7251	0.7951	0.8350	0.9121	0.8998
	SSE	0.5679	0.7983	0.8971	0.9095	0.8906
Elovich	$\alpha$ (g/mg.min)	12.4833	10.8541	7.8814	4.2145	1.4561
	$\beta$ (mg/g)	0.5225	0.7219	0.9921	1.0942	2.8403
	$R^2$	0.7452	0.8214	0.8831	0.8956	0.9016
	SSE	1.2389	4.5639	5.9086	7.4354	9.0342

## V. CONCLUSION

This present work was done to study the capacity of organo-clay compared to pristine clay to adsorb Ap and Cq from aqueous solution. Three adsorbent samples were used in this study, designated C1 for raw clay, C2 for treated clay, and C3 for organo-clay, which was synthesized by using citric acid to modify the C1 interlayer cations. XRD, SEM, and FTIR characterized both C1 and C3 to obtain physical and structural information on both, and the result revealed a chemical and physical modification of C1. Two process parameters were observed: initial adsorbate concentration and adsorbent/adsorbate contact times; the result revealed R% was inversely related to initial concentration for both Ap and Cq while the contact times increased and then equilibrated with respect to R%. Furthermore, the result showed that C3 adsorbs Ap and Cq

better than C2, and also, Ap was adsorbed better than Cq by C3. Both Langmuir and Freundlich models investigated the adsorption isotherm, and from the experimental data. The Langmuir model suitably described both Ap and Cq and showed maximum absorption capacity  $Q_{max}$  and  $K_L$  values for the removal of Cq by C2 are 54.945mgg<sup>-1</sup>, while the values for C3 are 84.034 mgg<sup>-1</sup>. Studied kinetic models were PFO, PSO, IPD, and Elovich on highest  $R^2$  and least SSE. The result showed that both Ap and Cq are best described by PSO kinetics. This study shows that organo-clay derived from kaolin is a suitable alternative in PACs removal from waste effluent.

## REFERENCES

- [1] V.H. John, R. Kirsten, L.B. Poul, H.C. Thomas, "Occurrence and Distribution of Pharmaceutical Organic Compounds in the

- Groundwater Downgradient of a Landfill (Grindsted, Denmark)," *Environmental Science & Technology*, Vol.29, No.5, pp.1415 – 1420, 1995.
- [2] S. Zuhlke, U. Dumbier, T. Heberer, "Detection and Identification of Phenazone-type Drugs and their Microbial Metabolites in Ground and Drinking Water applying Solid-Phase Extraction and Gas Chromatography with Mass Spectrometric Detection," *J. Chromatogr. A*, Vol.10, No.50, pp.201– 209, 2004.
- [3] K.E. Murray, S.M. Thomas, A.A Bodour, "Prioritizing Research for Trace Pollutants and Emerging Contaminants in the Freshwater Environment. *Environmental Pollution*, Vol.158 No.12, pp. 3462–3471, 2010.
- [4] L. Feng, E.D. Van Hullebusch, M.A. Rodrigo, G. Esposito, M.A. Oturan, "Removal of Residual Anti-Inflammatory and Analgesic Pharmaceuticals from Aqueous Systems by Electrochemical Advanced Oxidation Processes; A Review," *Chem. Eng. J.*, Issue.228, pp.944–964, 2013.
- [5] J.J. DiNicolantonio, J.H. O'keefe, C.J. Lavie, "The Benefits and Risks of Aspirin Use," *JAMA*, Vol.308, No.11, pp.1088-9, 2012.
- [6] M. Lindroos, D. Hörnström, G. Larsson G, M. Gustavsson, A.J. Van Maris, "Continuous Removal of the Model Pharmaceutical Chloroquine from Water Using Melanin-Covered Escherichia Coli in a Membrane Bioreactor," *J Hazard Mater.*, Vol.365, pp.74–80, 2019.
- [7] A.O. Dada, A.A. Inyinbor, S.O. Bello, B.E. Tokula, "Novel Plantain Peel Activated Carbon-Supported Zinc Oxide Nanocomposites (PPAC Zno NC) for Adsorption of Chloroquine Synthetic Pharmaceutical Used for COVID 19 Treatment," *Biomass Conversion and Biorefinery*, pp.1-13, 2021.
- [8] K. Mphahlele, K. Onyango, D. Mhlanga, "Adsorption of Aspirin and Paracetamol from Aqueous Solution Using Fe/N-CNT/B-Cyclodextrin Nanocomposites Synthesized via a Benign Microwave Assisted Method," *Journal of Environmental Chemical Engineering*, Vol.5 No.71, pp.1–12, 2015.
- [9] J. Žur, D. Wojcieszynska, K. Hupert-Kocurek, A. Marchlewicz, U. Guzik, "Paracetamol – Toxicity and Microbial Utilization. Pseudomonas Moorei KB4 as a Case Study for Exploring Degradation Pathway," *Chemosphere*, Issue.206, pp.192–202, 2018.
- [10] Y. Muhammed, "Biosafety and health molecular targets for COVID-19 drug development: enlightening Nigerians about the pandemic and future treatment," *Biosaf. Heal*, pp.1–8, 2020.
- [11] J.A. Hinson, A.B. Reid, S.S. McCullough, L.P. James, "Acetaminophen-induced Hepatotoxicity: Role of Metabolic Activation, Reactive Oxygen/Nitrogen Species, and Mitochondrial Permeability Transition," *Drug Metab. Rev.*, Vol.36, pp.805–22, 2014.
- [12] G. Dalgic, I. Turkdogan, K. Yetilmezsoy, E. Kocak, "Treatment of Real Paracetamol Wastewater by Fenton Process" *Chem. Ind. Chem. Eng Q.*, Vol.23, pp.29-35, 2016.
- [13] S. Hamoudi, M. Brahim, M. Boucha, B. Hamdi, J. Arrar, "Removal of Paracetamol from Aqueous Solution by Containment Composites," *Open Chemistry*, Issue.19, pp.49–59, 2021.
- [14] J. Sun, J. Wang, R. Zhang, D. Wei, Q. Long, Y. Huang, "Chemosphere Comparison of Different Advanced Treatment Processes in Removing Endocrine Disruption Effects from Municipal Wastewater Secondary Effluent," *Chemosphere* No.168, pp.1–9, 2017.
- [15] S. Bisarya, D. Patil, "Determination of Salicylic acid and Phenol (ppm level) in Effluent from Aspirin Plant," *Res. Ind. Iss*, Issue.38, pp.170– 172, 1993.
- [16] S. Chelliapan, T. Wilby, P. Sallis, "Performance of an Up-Flow Anaerobic Stage Reactor (UASR) in the Treatment of Pharmaceutical Wastewater Containing Macrolide Antibiotics," *Water Research*, Vol.40, pp.507-516, 2006.
- [17] V. Raki, N. Raji, A. Dakovi, A. Auroux, "The Adsorption of Salicylic Acid, 584 Acetylsalicylic Acid and Atenolol from Aqueous Solutions onto Natural Zeolites 585 and Clays: Clinoptilolite, Bentonite and Kaolin, Micropor," *Mesopor. Mater*, Vol.166, pp.185–194, 2013.
- [18] D. Dabi, S. Babi, I. Skori, "The Role of Photodegradation in the Environmental Fate of Hydroxychloroquine," *Chemosphere*, No.230, pp.268–277, 2019.
- [19] T. Heberer, K. Reddersen, A. Mechliniski, "From Municipal Sewage to Drinking Water: Fate and Removal of Pharmaceutical Residues in the Aquatic Environment in Urban Areas," *Water Sci. Technol.*, Vol.46, No.3, pp.81–88, 2002.
- [20] A. Joss, E. Keller, A. Alder, A. Gobel, C. McArdeall, T. Ternes, H. Siegrist, "Removal of Pharmaceuticals and Fragrances in Biological Wastewater Treatment," *Water Res.*, Vol.39, No.14, pp.3139-3152, 2015.
- [21] N. Kulik, M. Trapido, A. Goi, Y. Veressinina, R. Munter, "Combined Chemical Treatment of Pharmaceutical Effluents from Medical Ointment Production," *Chemosphere* Vol.70, pp.1525-1531, 2008.
- [22] D. Suman, Y. Anjaneyulu, "Evaluation of Biokinetic Parameters for Pharmaceutical Wastewaters using Aerobic Oxidation Integrated with Chemical Treatment," *Process Biochemistry*, Vol.40, pp.165-175, 2005.
- [23] W.H. Glaze, J.W. Kang, D.H. Chapin, "The Chemistry of Water Treatment Processes Involving Ozone, Hydrogen Peroxide and UV-radiation," *Ozone: Sci. Eng.*, Vol.9, pp.335–352, 1987.
- [24] Addamo M., Augugliaro V., Paola A., Garcia-Lopez E., Loddo V., Marci G., Palmisano L. "Removal of Drugs in Aqueous Systems by Photo Assisted Degradation," *Journal of Applied Electrochemistry*, Vol.35, pp.765-774, 2005.
- [25] K. Gupta, A. Suhas, "Application of low-cost adsorbents for dye removal - A review," *Journal of Environmental Management*, Vol.90, pp.2313–2342, 2009.
- [26] Z. Yu, S. Peldszus, M.H. Peter, "Adsorption Characteristics of Selected Pharmaceuticals and an Endocrine Disrupting Compound—Naproxen, Carbamazepine and Nonylphenol—on Activated Carbon," *Water Research*, Vol.42, pp.2873–2882, 2008.
- [27] Y. Hu, N.M. Fitzgerald, L. Guocheng, X. Xing, J. Wei-Teh, Z. Li, "Adsorption of Atenolol on Kaolinite" *Advances in Materials Science and Engineering*, Vol.1, pp.1-8, 2015
- [28] M. Houari, B. Hamdi, J. Brendle, O. Bouras, J.C. Bollinger, M. Baudu, "Dynamic Sorption of Ionizable Organic Compounds (IOCs) and Xylene from Water using Geomaterial-Modified Montmorillonite," *J Hazard Mater.*, Vol.147, pp.738–45, 2007.
- [29] Y. Seema, M. Datta, "In Vitro Sustained Delivery of Atenolol, an Antihypertensive Drug using Naturally Occurring Clay Mineral Montmorillonite as a Carrier," *European Chemical Bulletin*, Vol.2, No.11, pp.942–951, 2013.
- [30] P. Jozef-Bardzinski, "The Impact of Intermolecular Interaction between Quaternary Ammoniums Ions on Interlayer Spacing of Quat-intercalated Montmorillonite: A Molecular Mechanics and Abnatio Study," *Applied clay science*, Vol.95, pp.323 – 339, 2014.
- [31] M. Veiskarami, M.N. Sarvi, A.R. Mokhtari, "Impact of the Purity of Montmorillonite on its Surface Treatment with an Alkyl-ammonium Salt," *Applied Clay Science*. Vol.120, pp.111-120, 2016.
- [32] L. Betega, R.M. Ana, F.R. Diaz, "Organo-Clays: Properties, Preparation and Applications," *Applied Clay Science*, Vol.42, pp.8-24, 2008.
- [33] K. Mphahlele, S. Maurice, D.M. Sabelo., "Adsorption of Aspirin and Paracetamol from Aqueous Solution using Fe/N-CNT/b-Cyclodextrin Nanocomposites Synthesized via a Benign Microwave Assisted Method," *Journal of Environmental Chemical Engineering*, pp.1–12, 2015.
- [34] D.H. Lataye, I.M. Mishra, I.D. Mall, "Adsorption of 2-picoline onto Bagasse Fly Ash Fromaqueous Solution," *Chem. Eng.J.*, Issue.138, pp.35-46, 2008.
- [35] N. Yeddou, A. Bensmaili, "Kinetic Models for the Sorption of Dye from Aqueous Solution by Clay-wood Sawdust Mixture," *Desalination*, Issue.185, pp.499-508, 2005.

- [36] P. Anadão, L.R. Pajolli, E.A. Hildebrando, H. Wiebeck, "Preparation and Characterization of Carbon/Montmorillonite Composites and Nanocomposites from Waste Bleaching Sodium Montmorillonite Clay," *Adv Powder Technol.*, Vol.25, pp.926–32, 2014.
- [37] K.L. Salipira, R.W. Krause, B.B. Mamba, T.J. Malefetse, L.M. Cele, S.H. Durbach, "Cyclodextrin Polyurethanes Polymerized with Multi-walled Carbon Nano-tubes: Synthesis and Characterization," *Mater. Chem. Phys.* Issue.111, pp.21 8–224, 2008.
- [38] K.L. Salipira, B.B. Mamba, R.W. Krause, T.J. Malefetse, S.H. Durbach, "Carbon Nanotubes and Cyclodextrin Polymers for Removing Organic Pollutants from Water," *Environ. Chem. Lett.*, Vol.5, No.1, pp.13–17, 2007.
- [39] Y.M. Zheng, S.F. Lim, J.P. Chen, "Preparation and Characterization of Zirconium-based Magnetic Sorbent for Arsenate Removal," *J. Colloid Interface Sci.*, pp.22–29, 2009.
- [40] G. Annadurai, L.Y. Ling, J.F. Lee, "Adsorption of Reactive Dye from an Aqueous Solution by Chitosan: Isotherm, Kinetic and Thermodynamic Analysis," *J. Hazard. Mater.*, Issue.152, Vol.1, pp.337–346, 2008.
- [41] A.T. Aborode, "Adsorption of Ciprofloxacin HCl from Aqueous Solution using Activated Kaolin," *World Scientific News* pp.62-73, 2020.
- [42] S.Y. Adeyinka, T.P. Lekan, O.B. Esther, "Adsorption of Cadmium Ion from Aqueous Solutions by Copper-based Metal Organic Framework: Equilibrium Modeling and Kinetic Studies," *Applied water Science*, Vol.9, pp.106, 2019.
- [43] G. Ozturk, H. Silah, "Adsorptive Removal of Remazol Brilliant Blue R from Water by Using a Macroporous Polystyrene Resin: Isotherm and Kinetic Studies," *Environmental Processes*, Vol.84, pp.307-320, 2021.
- [44] E. Mekatel, S. Amorkrane, M. Trari, D. Nibou, N. Dahdouh, S. Ladjali, "Combined Adsorption/Photocatalysis Process for the Decolorization of Acid Orange 61," *Arabian Journal for Science and Engineering*, pp.1–12, 2019.
- [45] K.Y. Foo, B.H. Hameed, "Insights into the Modeling of Adsorption Isotherm Systems," *Chem. Eng. J.*, Issue.156, Vol.1, pp.2-10, 2010.
- [46] S. Qi, L.C. Schideman, "Isotherm for Activated Carbon Adsorption of Dissolved Natural Organic Matter in Water," *Water Res. Issue.42*. NO.13, pp.3353 – 3360, 2008.
- [47] A. Al-Wahbi, H. Dammag, "Removal of Methylene Blue from Aqueous Solution with Bentonite," *Eng. Sci.*, Vol.4, pp.30-53, 2011.
- [48] A. Fatima, K. Mustafa, K. Samer, T. Amin, K. Rafik, "Removal of Aspirin, Salicylic Acid, Paracetamol and *p*-Aminophenol by Advanced Membrane technology Activated Charcoal and Clay Micelles Complex," *Case Studies Journal*, ISSN: 2305-509X, 2015.
- [49] S.A. Hassan, J.I. Ibrahim, "Adsorption of Some Drugs onto Surface of Iraqi Kaolin Clay," *Pak. J. Chem.*, Vol.1, No.3, pp.132-137, 2011.
- [50] S. Dawood, K.T. Sen, "Removal of Anionic Dye Congo Red from Aqueous Solution by Raw Pine and Acid-treated Pine Cone Powder as Adsorbent: Equilibrium, Thermodynamic, Kinetics, Mechanism and Process Design," *Water Research*, Vol.46, pp.1933–1946, 2012.
- [51] A. Gürses, C. Dogar, M. Yalçın, M. Açıkıldız, R. Bayrak, S. Karaca, "The Adsorption Kinetics of the Cationic Dye, Methylene Blue, onto Clay," *J. Hazard. Mater.*, Issue.131, Vol.1-3, pp.217–228, 2006.
- [52] B. Nandi, K.A. Goswami, M.K. Purkait, "Removal of Cationic Dyes from Aqueous Solutions by Kaolin: Kinetic and Equilibrium Studies." *Appl. Clay Sci.*, Vol.42, pp.583–590, 2009.
- [53] A.A. Inyinbor, F.A. Adekola, G.A. Olatunji, "Kinetics, Isotherms and Thermodynamic Modeling of Liquid Phase Adsorption of Rhodamine B Dye onto Raphia Hookerie Fruit Epicarp," *Water Resour. Ind.*, Vol.15, pp.14–27, 2016.
- [54] J. Lin, L. Wang, "Comparison between Linear and Non-linear forms of Pseudo-first-order and Pseudo-second-order Adsorption Kinetic Models for the Removal of Methylene Blue by Activated Carbon," *Front. Environ. Sci. Eng.*, Vol.3, No.3, pp.320–324, 2009.